Invited paper

Application of liquid crystals in optical processing of optical signals

J. ŻMIJA, S. J. KŁOSOWICZ, J. KĘDZIERSKI, E. NOWINOWSKI-KRUSZELNICKI, J. ZIELIŃSKI, Z. RASZEWSKI, A. WALCZAK, J. PARKA

Institute of Applied Physics, Military University of Technology Warsaw, Poland

Physical principles of liquid crystal spatial light modulators are presented. The special attention is paid to optically addressed modulators. The most interesting systems are discussed in details including homogeneous nematic liquid crystals, polymer-dispersed liquid crystals, different modes of operation and main features of a construction. A brief description of liquid crystal holography and liquid crystal waveguides is also included.

1. Introduction

An optical processing of optical signals includes such processes as writing, analysis, transmission and storage of optical signals. These processes can be performed in as analogue as digital way. Analogue methods allow to provide very fast processing of a large amount of an information (up to 40^{12} bytes per second), but they are less accurate in comparison with digital methods. On the other hand, the latter are much more slower. Nowadays both methods are applied in alternative or complementary ways [1]. An important element of an each system of optical processing of information is an input module, which should transform signals to the proper form. Signals at the transducer input should be given in form of defined two-dimensional (or in special cases three-dimensional) amplitude-phase distribution of monochromatic (or quasi-monochromatic) optical field. Processed optical information is coded in form of parameters of coherent carrier wave which are changed in a proper way during modulation process.

A change of parameters of light beam performed to code certain information is called light modulation. This coded information is transmitted by light to a receiver, afterwards. An intensity of electric field of light wave (e.g., emitted by laser) E is given by the following expression:

$$E = \vec{e} E_0 \sin(2\pi\nu t + \phi) \tag{1}$$

where $\vec{e}$ stands for vector of polarization, ν for frequency, E_0 for amplitude, ϕ for phase and t for time. By changing amplitude, phase, frequency and polarization of light during signal transmission one can obtain light beam containing coded information.

Amplitude modulators usually consist of polarization (or phase) modulation system and a transducer which changes polarization modulation to amplitude modulation. The most effective way of light modulation is to change refractive indices of used material by electric or magnetic field.

In this way modulation is a physical phenomenon consisting in a transformation of certain quantities of one alternative electric signal (modulated or carrier signal) by the second (modulating) signal.

There are two groups of modulation techniques, namely continuous one and pulse one. A device in which primary signal containing an information overlapping a carrier light beam is called spatial light modulator - SLM [1]. In other words, in spatial light modulator a product C of two optical signals A and B is obtained. Strictly speaking in case of spatial light modulator all of those signals are functions of co-ordinates, e.g., C(x,y) = A(x,y) B(x,y).

The feature called internal optical parallelism is

* address for correspondence: Institute of Applied Physics, Military University of Technology, 01-489 Warszawa, ul. S. Kaliskiego 2, phone: +48-22 685 97 31, fax: +48-22 685 91 09, e-mail: raszez@wat.waw.pl

important for optical information processing. The elegant but historical illustration of this idea is optical Fourier transformation of a distribution of planar electric field. In these terms Fraunhofer diffraction can be treated as a Fourier transformation of the field image [2].

An application of coherent light sources made Fourier optics to be very important technique of image filtering and processing [3]. Light beams with different wave vectors can independently exist in the same areas of space. This internal parallelism makes possible to apply devices modifying amplitude, phase and polarization of a wave-front as functions of time and position. An information obtained in this way can be adopted as for static images (photographs, patterns) as for dynamic processing of optical information. SLM are used for an introduction and storage of an information, an accomplishment of logic operations and a construction and reproduction of holograms in real time [4,5]. It seems that the development of optical information processing is now limited namely by possibilities of SLM's.

An important group of SLM's, with large application possibilities, uses electro-optical properties of liquid crystals – LC to write an information. Such modulators are called LCSLM [6] and usually consist of LC film and photoconductor layer. As photoconductors, Se, Si in form of single-crystalline plates and amorphous layers, single crystals of CdS, GaAs, Bi_{12} Ge O_{20} and organic compounds have been adopted.

All main thermotropic LC phases and most of known electro-and thermo-optical effects have been adopted for LCSLM construction [7,8].

Nematic LC phase (NLC) exhibits orientational molecular arrangement. In case of several smectic LC (SmLC) also long-distance positional molecular arrangement is observed. LC films aligned by suitable treatment of bordering surfaces exhibit optical properties similar to those of plates cut out from uniaxial single crystals, LC birefringence does not exceed 0,2, however. Fluidity of LC medium and thickness of LC film, usually up to a dozen or so micrometers allow to drive LC optical axis by voltages lower than 10 V. Reorientation (switching) times at room temperature are from 1ms to 10 ms, depending on used effect. A possibility to drive LC optical axis by means of electric field is the base for electro-optical effects observed in LC.

In spite of rather low response time in comparison with typical electro-optical crystals, LC are often used in SLM for the following reasons [6]:

1. Flexibility of application

This term means that it is easy to choose the proper SLM geometry and optical properties for a given application.

2. Effective action for low driving voltages and power consumption

This feature is especially important for portable devices. Low power consumption is the result of use field effects to control optical properties of LC. Low level of driving voltage is the effect of small thickness of LC layer and enables to operate with conventional integrated circuits.

3. Simple and convenient technology

Technology required for manufacturing of LC transducers is much less complicated and „microscopic" than in case of semiconductor technology. Because used electro-optical effects are observed in thin layer of LC the whole transducer can be flat. There is not significant limitation concerning an aperture of LC transducers as in case of solid materials. This feature allows mass production of devices, even complicated ones. Moreover there are many different technologies and manufacturers of LC transducers.

Due to the above properties LC are widely used for information display and processing of optical signals. The important feature of optical devices is internal parallel optical processing, which means a possibility to process different signals in the same time, e.g. in case of optical Fourier transformation. Using LC one can successfully accomplish this requirement and construct devices for image filtration and processing.

Below LCSLM are discussed in details. The special attention is paid to the optically addressed SLM – OASLM, however electrically addressed SLM – EASLM are also described. In addition, LC real-time holography is described because in fact holographic image of Fourier transform is obtained in SLM's. LC waveguides are also briefly presented because they give new possibilities as additional devices to construct SLM's. On the other hand, typical fiber optic devices are not mentioned due to extensive literature of this subject.

2. Liquid-crystalline spatial light modulators (LCSLM)

LC devices, as it was underlined, are relatively cheap, simple and flexible from application point of view. For this reason they are intensively studied recently.

LCSLM can be divided into two essential groups. The first one are optically addressed modulators (OASLM), in which two-dimensional (2-D) optical image is present at the input, while the output is modu-

lated by input signal and/or reading beam (see Fig. 1 a and b). The second group comprises electrically addressed modulators (EASLM) with matrix construction, in which mixed electric and optical processing of an input signal is adopted (see Fig. 1c). 2-D input image (transmissive or reflective) is modulated by a voltage applied to each pixel of a matrix. EASLM are often used as input devices for images generated or saved in optical systems for further processing. All LC image projection systems are in fact EASLM.

The important feature of SLM's is a possibility to control them by a computer either directly (EASLM) or via image source, e.g., CRT (OASLM).

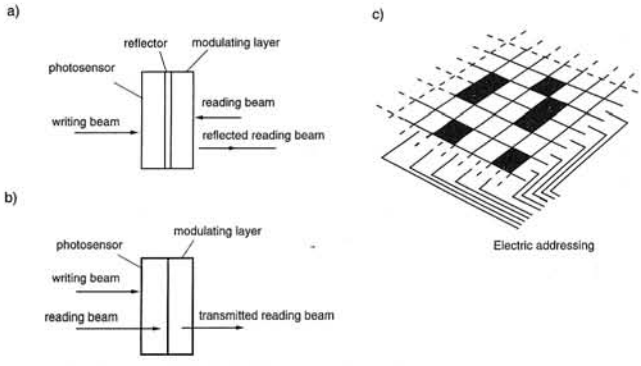

Fig. 1. The principle of an action of OASLM: (a) reflecting mode and (b) transmitting mode and EASLM (c) transducers.

The essential function of SLM is multiplying modulation. Reading beam with an amplitude of A_R (x,y) is multiplied by modulation functions (either transmission or reflection ones) which can be complex functions in general. In case of OASLM shown in Fig. 1a, in which input and output are separated by dielectric mirror, a reflection coefficient R (x,y) is a function of written image A_W (x,y). If R is proportional to A_W, the simple multiplying of an image in time is obtained. Using reading beam of suitable intensity one can obtain image amplification. If reading beam is coherent while writing one is incoherent a transformation of an image is possible. Operations of subtraction and dividing are also possible. Operation of multiplying is used for numerical multiplication of vectors and matrices [9], which was adopted for a construction of neural networks and dynamic phase optical connections [10-12].

Typical dependence between input field and modulation function is nonlinear multiplying, which allows parallel optical processing of a function. For instance, function of binary modulation can be applied for a threshold operation by means of continuous change of a grey-scale while two grey states are chosen in advance and carefully controlled. Such effects are used complementary for parallel optical processing (POP), accomplishment of neural networks and imaging of Boolean algebra. These possibilities are limited by bi- and multistability phenomena, which in turns can be adopted for a construction of memory devices, e.g., SLM's using memory effects observed in ferroelectric smectic LC [13].

The very important application of SLM's is a location and recognition of light sources. Usually a tandem of SLM's is used for this purpose. At the first of them Fourier transform of observed object is done while on the second one Fourier transform of an etalon image is performed. If a these transforms coincide a correlation signal is obtained. Such devices are often called light correlators.

2.1. Liquid-crystalline TV electrically addressed light modulators (LCTV EALSM)

The mass production of 2-D matrix LC light valves for video displays is a potential source of cheap electrically driven SLM's. LC devices acting simultaneously with CRT have been studied long time ago [14], but practical solutions have been known since eighties. LCTV displays have been designed for other purposes than optical information processing and have rather low optical contrast ratio (a_k ~1:10) and speed (~30 frames per second). On the other hand they are very flexible from application point of view and compatible with computers. Exactly these two features make possible to use LCTV also for a processing of optical information. LCTV have been applied as optical input devices, logic elements, computer 2-D phase generators with holographic writing, filters and for tracking many different objects in real time. Liv and Chao [15] discussed characteristics of LCTV SLM from optical data processing point of view. Their results are gathered in Table 1 as typical for devices of an older generation.

Characteristics of transmission of devices of such kind have been comparable with those of magneto-optical SLM's.

2.2. Optically addressed spatial light modulators (OASLM)

OASLM are useful modulating devices using optical parallelism in writing mode [16]. Such a device can be described as a transparent capacitor made of con-

Table 1. The comparison of properties of different LCTV SLM

Model Characteristic	Radio Shack (black-and-white) passive matrix	Epson (colour) active matrix	Citizien (colour, filters) passive matrix
Aperture [cm × cm]	4,4 × 5,4	2,9 × 3,8	2,3 × 2,3
Number of pixels	120 × 146	220 × 240	220 × 648
Dimensions of a pixel [μm × μm]	366 × 370	131 × 158	104 × 49
Glass flatness (λ = 633 nm)	6	·11	6
Max contrast without space filtering with space filtering	6 > 10	11 > 30	6 > 10
Grey-scale levels	< 6	~ 6	> 6
Max. transmission of polarized light (T = 25°C, λ = 633 nm)	~50% (built-in polarizer)	~7% (outside polarizer)	~7% (outside polarizer)
Transmission band	visible to IR	visible	visible to IR
Input device	TV camera or computer	TV camera or computer	TV camera or computer
Addressing	matrix	active matrix (TFT)	matrix
Addressing speed [frames/s] at 25°C	30	30	30
Relaxation time of a pixel [ms]	~30	~100	~10
Power consumed [W]	0,33	1,1	0,87
Temperature of work/storage [°C]	5-40/-20- +60	5-40/-20 +60	5-40/-20 +60
Total weight [g]	~300	450	~450

ducting oxide layers deposited on glass substrata. This capacitor contains LC film 1 – 10 μm thick, which plays a role of electro-optical readout layer, photosensitive layer (photoreceptor) and sometimes dielectric reflector acting as optical blocking layer between input and output. As a photoreceptor, photoconductive layer, e.g. Se or CdS, photovoltaic layer or plate cut out semiconductor single crystal can be used. Photoreceptor thickness should be minimized to increase SLM spatial resolution. Input optical image activates photoreceptors which generate suitable distribution of charge. This distribution changes electric field applied to LC, hence a distribution of director in LC layer. Exactly for this reason LC cell modulates readout beam passing through. A combination of reading and writing modes defines sensitivity, resolution and response time of SLM. Response time is limited also by light intensity.

Due to an application of an isolator which blocks light between input and readout beams OASLM can amplify incident beam when readout source of large intensity is applied, moreover can convert incoherent light to coherent light. Without dielectric mirror OASLM as nonlinear optical element is especially useful in form of matrix SLM to prepare images with periodic structures changing transversal space frequencies.

2.2.1 Foundations of LC OASLM action

From macroscopic point of view aligned NLC exhibits properties of uniaxial crystal. Incident light is divided into ordinary and extraordinary beams in each direction except optical axis. Both beams have different velocity of propagation and are polarized in perpendicular planes. In Fig. 2 plane-parallel NCL birefringent sample – PD is presented; optical axis A of this sample forms angle of β with bordering surfaces.

Wide parallel beam of unpolarized monochromatic light with planar phase surface Σ incident normally to PD cell. In figure only one light ray S of this beam is

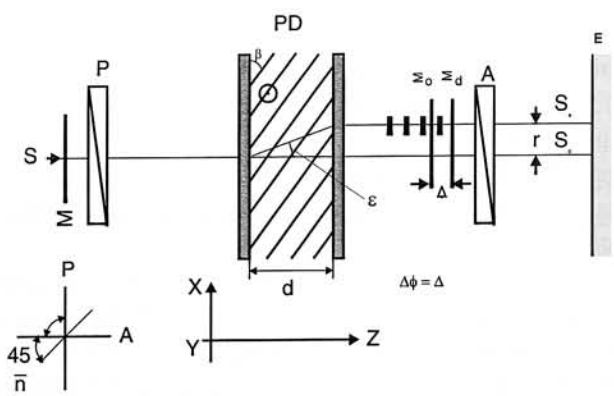

Fig. 2. An illustration of NLC birefringence.

presented. In PD incident beam is divided to ordinary beam S_0 passing through PD without refraction and extraordinary beam S_e refracted to the direction of optical axis because NLC are usually optically positive ($n_e > n_0$). After passing the cell both beams are parallel and lie in the plane determined by optical axis and normal to the bordering surfaces of PD. This plane is therefore the main cross-section of aligned PD. There are infinite number of main cross-sections because optical axis can be attached to each point inside crystal. Beams S_0 and S_e are linearly polarized in perpendicular planes. Oscillations of light (electric) vector of an extraordinary beam take place in main cross-section plane, while those of ordinary beam in plane perpendicular to this cross-section. Due to different velocities in PD a difference of optical paths Δ is observed between both beams after passing PD:

$$\Delta = AB \cdot n'_e - AB \cdot n_0 \approx (n'_e \cdot \cos\varepsilon - n_0) \cdot d \quad (2)$$

where stands for an angle between S_0 and S_e beams in PD cell, d for cell thickness, n_0 and n_e for refractive indices of ordinary and extraordinary beam, respectively. Index n_0 is constant while n'_e depends on an angle. Knowing the highest value of n_0, i.e. main refractive index of an extraordinary beam, one can calculate n'_e from the following dependence [17, 18]:

$$n'_e = \frac{n_0 n_e}{\sqrt{n_e^2 \sin^2\beta + n_0 \cos^2\beta}} \quad (3)$$

Assume, that incident light is broad planar wave with wave-plane Σ. After passing PD this wave is divided into two ones with wave-planes Σ_o i Σ_e, respectively. There are separated as longitudinally (along the direction of light propagation) by a length of Δ described by an equation (2) as transversely by a length of r expressed as:

$$r = d \cdot tg\varepsilon = d \frac{(a^2 - b^2)\sin 2\beta}{(a^2 + b^2) + (a^2 - b^2)\cos 2\beta} \quad (4)$$

where $a = n_e^{-1}$ and $b = n_0^{-1}$

At a first sight those light waves should interfere in the area of superposition of wave-planes Σ_0 i Σ_e (see Fig. 2). Such an interference does not take place, however, because ordinary and extraordinary waves, despite they origin from the same original wave S, are incoherent, moreover they are linearly polarized in perpendicular planes. Even if turned to the same polarization by means of a polarizer P placed behind or in front of the PD they do not interfere, because they remain incoherent. In this way, there is a classic birefringent inteference system, sometimes called a polariscope.

Several electro-optical effects have been successfully applied for LCSLM construction. In case of NLC usually one of the following effects is adopted (see also Fig. 3 and 4):

- electrically induced splay deformation of initially homogeneous dielectrically positive ($\Delta\varepsilon > 0$) nematic film, sometimes called S-effect,
- electrically induced bend deformation of initially homeotropic dielectrically negative ($\Delta\varepsilon < 0$) nematic film, sometimes called B-effect,
- twisted-nematic effect (TNE) of dielectrically positive nematic film.

Two former effects are called electrically controlled birefringence (ECB). Electric field changes continuously birefringence of plane-parallel NLC cell. In the TNE effect optical activity of nematic cell can be controlled in a continuous way (see Fig. 4). Above effects are often called Freederiksz's effects.

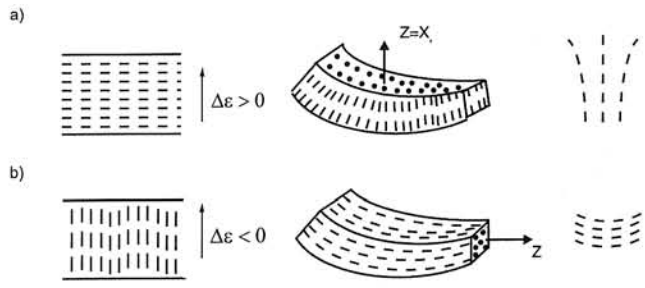

Fig. 3. Schematic presentation of ECB electro-optical efects in nematic LC a) S-effect (splay deformation), b) B-effect (bend deformation).

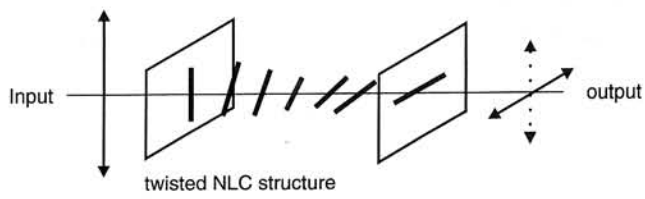

Fig. 4. Schematic presentation of electro-optical effect of twisted nematic – TNE; bars represent LC director.

In case of ECB effects a transmittance of a studied cell is defined by the following formula:

$$T = T_0 \, \grave{a} \, \sin^2 2\beta \cdot \sin^2\left(\frac{\Delta\Phi}{2}\right) \quad (5)$$

If an angle between polarization vector of a an incident light and NLC director is $\beta = 45°$ then:

$$T = T_0 \cdot \sin^2\left(\frac{\Delta\Phi}{2}\right) \tag{5a}$$

Phase shift $\Delta\Phi$, between ordinary and extraordinary beams introduced as the effect of passing through a NLC cell can be found from the following equation:

$$\Delta\Phi = 2\arcsin\sqrt{\frac{T}{T_0}} \tag{6}$$

where T_0 stands for an intensity of incident linearly polarized light, while T for an output light intensity.

Local refractive index can be calculated from the following formula:

$$n(z) = n(\theta) = \frac{n_0 \cdot n_e}{\sqrt{n_e^2 \sin^2\theta(z) + n_0^2 \cos 2\theta(z)}} \tag{7}$$

Hence the effective refractive index of extraordinary beam can be expressed as follows:

$$n_{eff} = \frac{1}{d}\int_0^d \frac{n_0 \cdot n_e}{\left[n_e^2 \sin^2\Theta(z) + n_0^2 \cos^2\Theta(z)\right]^{1/2}} \tag{8}$$

For this reason phase shift between ordinary and extraordinary beams after passing a sample d thick is:

$$\Delta\Phi = \Phi_\varepsilon - \Phi_0 = \frac{2\pi}{\lambda}\int_0^d \frac{n_0 \cdot n_e dz}{\left[n_e^2 \sin^2\Theta(z) + n_0^2 \cos^2\Theta(z)\right]^{1/2}} - n_0 d = \frac{2\pi}{\lambda}\langle \Delta n(z)\rangle \tag{9}$$

where $\Theta = \Theta$ (E,z); $\Delta n = n_e - n_0 = n_{||} - n_\perp = \Delta n$ (E,z) and $\Delta\Phi = \Delta\Phi$ (E), respectively.

Another conception is a change of phase shift:

$$\Delta\Phi_1 = \Delta\Phi_{max} = \frac{2\pi}{\lambda}\left[n_e d - \int_0^d \frac{n_0 \cdot n_e dz}{\sqrt{n_e^2 \sin^2\Theta(z) + n_0^2 \cos^2\Theta(z)^{1/2}}}\right] \tag{10}$$

where $\Delta\Phi_1 = \Delta\Phi(E = 0) - \Delta\Phi(E) = \Delta\Phi(U = 0) - \Delta\Phi(U)$, respectively.

It results from an Eq. (9) that the largest phase shift between ordinary and extraordinary beams $\Delta\Phi_{max}$ can be obtained if $\Phi = \Phi_0$

$$\Delta\Phi_{max} = \frac{2\pi}{\lambda} \cdot d(n_e - n_0^{zn}) = \Delta\Phi_0 \tag{11}$$

Function (9) has got extrema if the following identity is fulfilled:

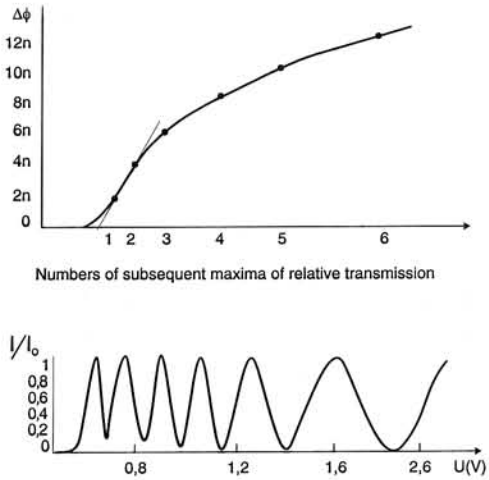

Fig. 5. The examples of dependencies of relative transmission T/T_0 and phase shift $\Delta\Phi$ of homeotropic cell filled with nematic LC upon applied voltage U (B-effect). Cell thickness d = 38 μm.

$$\Delta\Phi_0 = m\pi \quad (m = 1, 2, 3, ...) \tag{12}$$

A condition (12) describes a number of transmission extrema $n = \frac{\Delta\Phi_0}{\pi}$ for a cell filled with NLC, as it is shown in Fig. 5, in which exemplary oscillation dependencies of relative intensity of radiation transmitted by the cell vs. applied voltage are presented. In the same figure phase shift $\Delta\Phi$ between ordinary and extraordinary beams for transmission of a given cell is presented.

2.2.2. Optimization of LC mixture and a construction of LC OASLM

The input dependence of a voltage applied to the cell (U_{LC}), related to the total voltage (V), and relative light intensity I to the threshold intensity of photosensitivity is expressed as [22]:

$$\frac{U_{LC}}{U} = a + b\ln\left(\frac{I}{I_{th}}\right) \tag{13}$$

where a and b stand for parameters dependent on resistivity and capacitance of LC and MDS-LC structure (Metal – Dielectric Semiconductor – LC, see Fig. 6.)

The intensity transforming an image is described in each point of SLM aperture by the following equation:

$$I_{out} \sim \Delta \sin^2 (\Delta\Phi (U_{LC})/2 \tag{14}$$

It has been proved, that image contrast ratio and intensity of spatial image spectrum are defined by phase shift of extraordinary beam due to differentiated illumination (see Fig. 7).

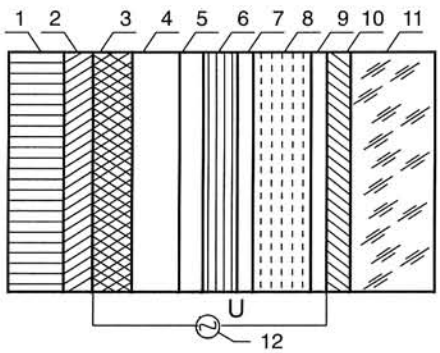

Fig. 6. A scheme of reflective LC OASLM using MDS-LC structure; 1 - selfoc, 2,10 – electrodes (indium – tin oxide), 3 – dielectric mirror (optical glue or SiO), 4 – photoconductor (GaAS or α Si:H), 5 – light blocking film (CdTe), 6 – dielectric mirror, 10 – SiO_2 – TiO_2 films, 7,9 – aligning films, 8 – LC, 11 – glass plate, 12 – generator.

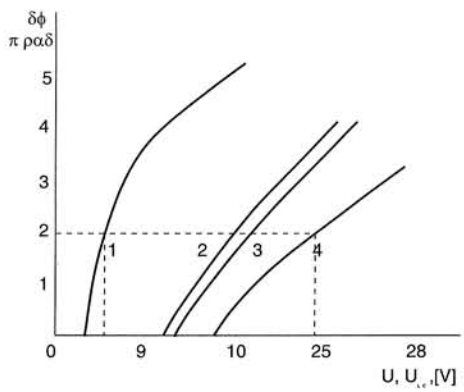

Fig. 7. The dependence of phase shift on LC film (1) on SLM driving voltage – U (2, 3, 4) for input intensity I = 0,1 (2), 0,01 (3) and 0 (4) mW/cm^2. Dashed lines allow to calculate a U_{LC}/U ratio for constant phase shift.

$$\delta\Phi = \frac{2\pi d}{\lambda} \frac{\delta_e}{\delta U_{LC}} \left(a + bln\frac{I}{I_{th}}\right)\left(\frac{U - U_{th}}{a + bln\frac{I}{I_{th}}}\right) \tag{15}$$

where δ_{ne} is a change of extraordinary refractive index for $U_{LC} > U_{th}$ (threshold voltage).

$$\delta\frac{n_e}{\delta U_{LC}} = \frac{1}{U_{th}} \frac{\Delta n(n_e + n_{0)}}{n_0^2} \left(\frac{K_{33}}{K_{11}} + \frac{\Delta\varepsilon}{\varepsilon\perp}\right)^{-1} \tag{16}$$

where K_{11} i K_{33} stand for elastic constants for splay and bend deformations, respectively, $\Delta E = E_n - E$ where E_{11} and E stand for dielectric constants parallel and perpendicular to LC director, respectively, $\Delta = n_e - n_0$ for birefringence.

For low input intensity ($I/I_{th} - 1 = \delta I < 1$) the expression (15) takes the following form:

$$\delta\Phi = \frac{2\pi d}{\lambda} \frac{\delta_e}{\delta U_{LC}} (a + bln\delta I) \frac{U - U_{th}}{a + bln\delta I} \tag{17}$$

The maximum value of $\delta\Phi$ depends on input image contrast ratio k:

$$\delta\Phi = \frac{4\pi d}{\lambda} \frac{\delta n_e}{\delta U_{LC}} bUlnk \tag{18}$$

For a low contrast ratio one can obtain:

$$\delta\Phi = \frac{4\pi d}{\lambda} \frac{\delta n_e}{\delta U_{LC}} bUln\,(k - 1) \tag{19}$$

It results from the above equation, that the contrast ratio of a transmitted image increases with an increase of a steepness of static electro-optical characteristics and a portion of a total voltage applied to LC film. For ECB effect characteristic steepness is expressed by the $\delta n_e/\delta U_{LC}$ ratio. Information characteristics of a SLM depend preferably on properties of LC film and should be optimized from these properties point of view.

Optical response of LC film for S- and B-effects is described by the following coefficient [20]:

$$M_2 = \frac{\lambda d}{\tau_\pi} \frac{U_{th}}{\Delta U_{th}} \tag{20}$$

where τ_p and ΔU_{th} stand for switching time and a change of an applied voltage responding phase shift $\Delta\Phi = \pi$. The dependence M_2 upon U_{LC} has a maximum for $U_{LC} \approx 1{,}5$–$2\ U_{th}$. In case of S- and B-effects, M_2 for $U \to U_{th}$ can be expressed as:

$$M_s = \frac{K_{11}}{\gamma_1} \Delta n \left(\frac{K_{33}}{K_{11}} + \frac{\Delta\varepsilon}{\varepsilon\perp}\right)^{-1} \tag{21}$$

$$M_B = \frac{K_{33}}{\gamma_1} \Delta n \left(\frac{K_{11}}{K_{33}} - \frac{\Delta\varepsilon}{\varepsilon\perp}\right)^{-1} \tag{22}$$

where γ_l i η_B stand for viscosity coefficient for S- and B-effect, respectively.

The dependence of $\Delta U_{LC}/\Delta U_s$ ratio (increase of a voltage applied to LC film – ΔU_{LC} to increase a voltage at photoconductor film ΔU_s) is illustrated in Fig. 8. Similar dependencies for relative changes of the response Dd/DU_s are shown in Fig. 9.

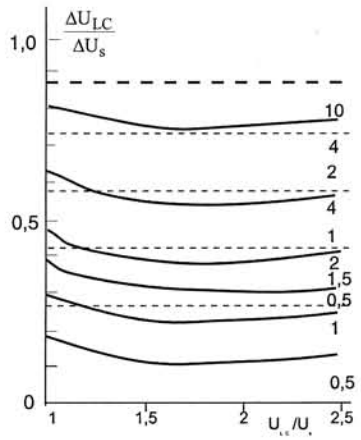

Fig. 8. The $\Delta U_{LC}/\Delta U_S$ dependence (electric SLM response) upon reduced voltage at LC film calculated for different thickness ratios d_{lc}/d_D and $\Delta\varepsilon = 2$ (---) or 10,7 (—).

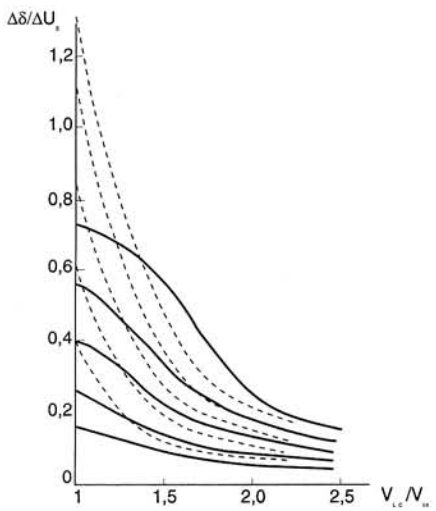

Fig. 9. Relative optical response $\Delta d/\Delta U_S$ as a function of relative voltage V_{LC}/V_{th} calculated for different system parameters (see Fig. 8).

Knowing characteristics of photoconduction changes vs input light intensity one can calculate a transformation of the original image by:

$$\delta = \frac{\Delta\Phi_{max} - \Delta\Phi}{\Delta\Phi_{max}} \Delta\Phi_{max} = \frac{2\pi d \Delta n}{\lambda} \qquad (23)$$

Values of $\Delta V_{LC}/\Delta V_{th}$ and $\Delta d/\Delta U_S$ ratios increase with an increase of thickness ratio d_{LC}/d_S and a decrease of LC dielectric permittivity. A value of $\Delta d/\Delta U_S$ decreases with an increase of K_{33}/K_{11} ratio for $V_{LC}/V_{th\,LC} = V_{th}$ and slowly increases for $V_{LC} = 2\,V_{th}$.

To increase a response one should decrease thickness of dielectric films (i.e., applied oxide films) and relative dielectric anisotropy $\Delta\varepsilon/\varepsilon_\perp$. The latter means that mesogens with transversal dipole moments which cause an increase of $\varepsilon_\perp$ should be introduced into LC mixture. The value of K_{33}/K_{11} ratio should be also optimized.

An application of LCSLM requires different switching times in case of different devices for optical processing. For instance, when used as input elements they should be very fast, while used for subtraction and storage of images they should exhibit optical memory effects.

The highest signal has been observed for kH frequencies. In case o low frequencies (~ 10 Hz) MDS – NLC structure exhibits linear electro-optical response to driving voltage due to ferroelectric efect.

Taking above into account one can optimize LC materials used in SLM. Usually so called four-bottle systems of LC materials which allow for easy preparation of proper LC mixture are manufactured for this purpose.

The example of essential parameters of LC SLM using different photosensitive materials are gathered in Table 2. In Table 3 information characteristics of LC SLM using photosensitive film of GaAs and two different LC mixtures are given. The scheme of projection system using this solution is presented in Fig. 10.

Table 2. Properties of LC SLM using different photosensitive materials

Parameter	a-CdTe	a-Si:H	GaAs
Threshold sensitivity [μW/cm²]	1	0.1	0.1
Switch-on time [ms]	200-400	5-200	10-50
Switch-off time [ms]	200-400	5-200	10-50
Spectral sensitivity band [nm]	550-900	550-900	550-1000
Diffraction efficiency η_{max} [%]	0.5	5	10
Spatial frequency ν [nm⁻¹] $\eta = 0{,}01\ \nu_{max}$ $\eta = 0{,}01\ \nu_{max}$	 160 80	 120 50	 140 55
Resolution for 0,5 of maximum contrast ratio [mm⁻¹]	30	25	25

Table 3. Parameters of LC SLM for different LC materials. U_{SLM} = 70V, I_{in} = 32 W/cm^2, full contrast change ($\delta\Phi = i\pi$) [19]

Parameter	ZhKS – 1282 mixture	UK – 11 mixture
Response time for optical pulse [ms]	120	12
Relaxation time [ms]	180	20
Contrast ratio of transformed image	65	80
Number of distinguishable elements	1250 × 1250	890 × 890
Capacity of data transmission [bit/s]	6,5 × 10^7	4,43 × 10^8

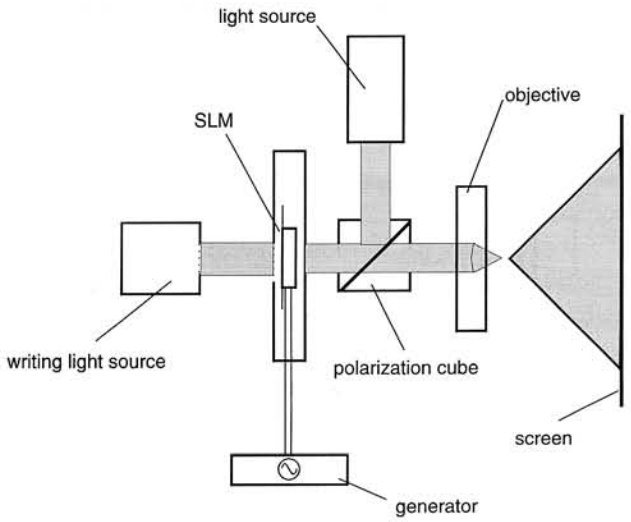

Fig. 10. The scheme of LC OASLM used for image projection.

2.2.3. Selected applications of LC OASLM

In classic OASLM developed by Hughes [21] CdS film 15 μm thick, optically isolated from read-out beam by dielectric mirror and CdTe light blocking film has been adopted as a photosensitive element. The device of this kind works in reflective mode with different configurations of LC optics (director field) for information read-out. In basic configuration NLC film works in mixed mode of TN effect if bias voltage is not applied. An applied voltage unwinding structure and allows to drive birefringence. If pretilt of LC (an angle between bordering surface and neighbouring director) is sufficiently high (45°), well-defined off-state and switching threshold can be obtained. Such a configuration has a relaxation time (return to off-state) order of 10 ms. Fast response can be obtained using configuration in which director field is stabilized by strong anchoring on bordering surfaces. In [22] ZnS (as CdS $A^{II}B^{VI}$ type semiconductor) sensitive to UV radiation

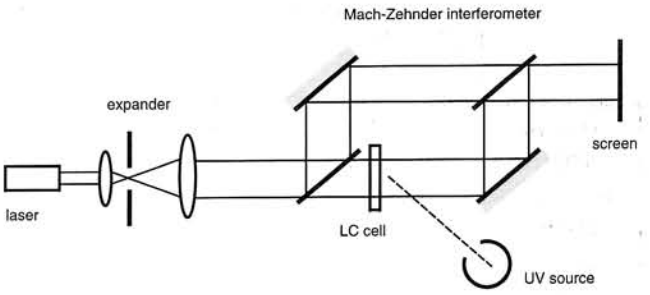

Fig. 11. The scheme of Mach-Zehnder interferometer with OASLM modulator.

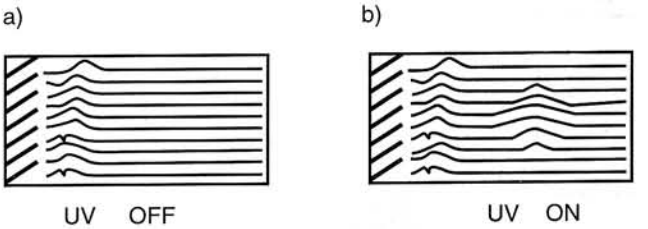

Fig. 12. Interference images; (A) without UV light, (B) with UV illumination.

has been applied. Obtained modulator has been studied in Mach – Zehnder interferometer configuration by He-Ne laser beam (see Fig. 11). Obtained interference images are shown in Fig. 12.

The main disadvantage of $A^{II}B^{VI}$ based OASLM is rather long response time (~10 ms), due to wide energetic gap and long lifetime of trapped charges. For this reason many new photosensitive materials and LC electro-optical effects have been introduced into OASLM In Table 4 a device of Japanese company Hamamatsu Corp.is presented. Biometric application of OASLM developed by this company is given in Fig. 13 [23].

Nippon Telegraph & Telephone Corp. developed a system of image transmission directly by optic fibre without a necessity to transform them into electric signals [24]. This system uses ferroelectric smectic LC (FLC SLM) with parallel amplification of stored images. Modulator acts as a phase coupled mirror reflecting incident beam with phase reversion. It allows for a correction of noise introduced by a fibre. In Fig. 14 the principle of this modulator is presented. Transmitted light wave carries an information phase-disturbed in an optic fibre, while reference wave carries an information to modulator. Phase noises are eliminated as a result of interference of both beams.

Table 4. Parameters of OASLM manufactured by Hamamatsu Corp.

	Twisted NLC	Homogeneous NLC	Ferroelectric LC
Active area [mm^2]	18 × 18	18 × 18	18 × 18
Resolution [lp/mm]	50	50	100
Response time [ms]	$T_r = 50$ $T_f = 40$	$T_r = 50$ $T_f = 40$	$T_r = 0{,}06$ $T_f = 0{,}04$
Contrast ratio	100:1	2π	30 : 1
Memory	—	—	Bistable
Image polarity	—	—	Bipolar
Modulation	Intensity	Phase-intensity	Intensity

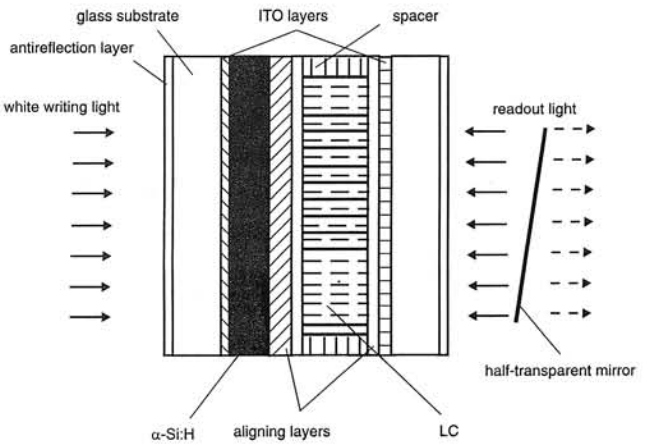

Fig. 13. A construction of OASLM manufactured by Hamamatsu Corp.

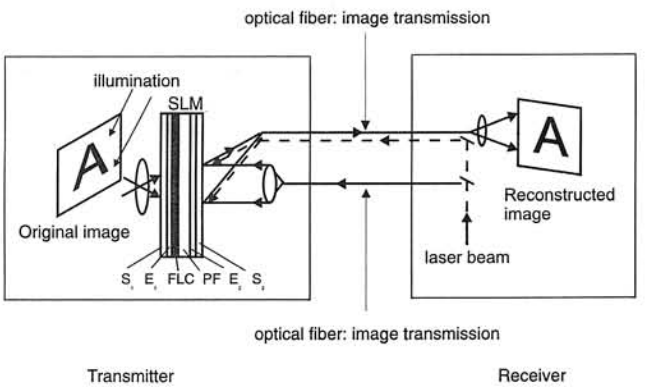

Fig. 14. Interference of transmitted and reference beams in SLM decreasing phase noises, PF photoconductor, E – electrodes, S – glass substrata, FLC – ferroelectric LC.

In [25] a construction of SLM using polymer-dispersed LC – PDLC and photoconductive layers of $Bi_{12}SiO_{20}$ (BSO) has been described. This system transformed poor output image to excellent projection image. The construction and mode of work of this modulator is given in Fig. 15. PDLC and BSO films were 10 and 250 μm thick, respectively. Typical static electro-optical characteristic of PDLC film is shown in Fig. 16 [26]. In case of conventional LC SLM more than 50% of read-out light is lost at a polarizer, while PDLC based modulator does not require polarizer at all. The modulator of this kind with threshold resolution 3650 Ip/m has been constructed. On this base projection system has been developed (see Fig. 17) in which LC active matrix transducer has been used as input image element and 1 kW xenon lamp as a projection light source. The green image with diagonal of 60'', high contrast (100 : 1) and luminance 1500 lm has been obtained. Systems of this kind can be applied at command stations.

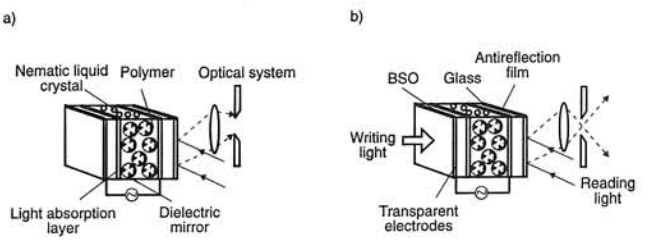

Fig. 15. Schematic view of polymer-dispersed liquid crystal light valve (PDLCLV); a) without illumination, b) with high level of illumination.

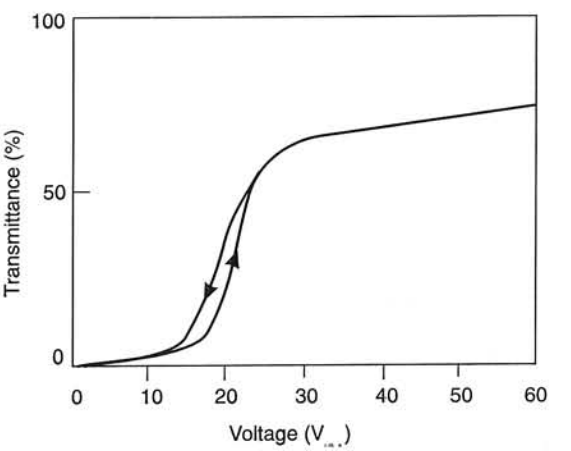

Fig. 16. The dependence of transmission of PDLC cell 10 m thick upon applied voltage.

Few interesting solutions have been presented in [27]. Transducer applied to change of incoherent to coherent image can be applied to fix a location and orientation of three-dimensional objects, moreover, for identification and tracking trajectory of object in real time (e.g., missile or aircraft). An image of an object illuminated by white light is projected at transducer

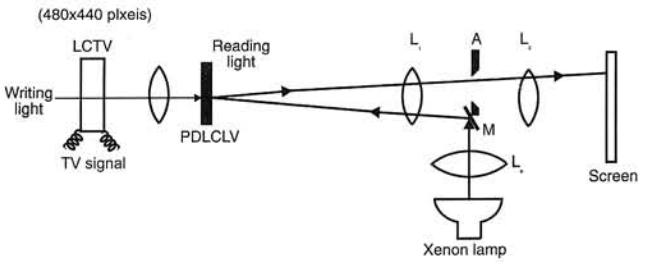

Fig. 17. Schematic view of monochrome projection display using PDLCLV and liquid crystal active matrix at the image input, M – semi-transparent mirror, L - lenses.

input. Then obtained output signal (deformation of LC structure) is modulated by coherent light beam which together with reference beam is used to form a hologram of Fourier transform of the object. Hologram registered at photographic plate is then used as a filter allowing to detect correlation signal in output plane of an optical system. For stationary objects detection can be performed, e.g. by vidicon camera, while obtained image is presented by TV monitor.

There have been studies on the application of image transducer to compress radar signals and process data concerning a position and velocity of tracked objects. Antenna signal is mixed in radiolocation receiver with heterodyne signal to adjust it to work frequency of the system of pulses compression.

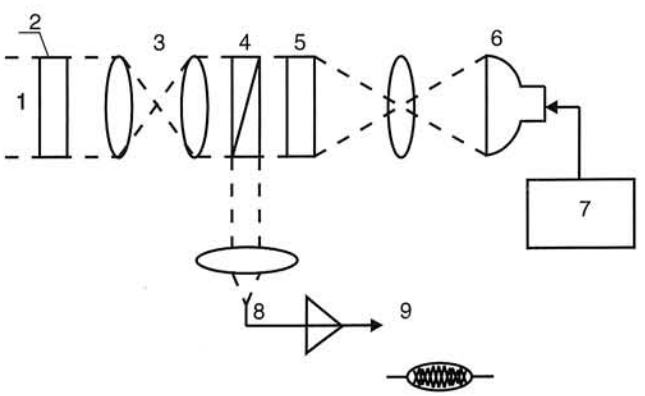

Fig. 18. Scheme of a construction of an image collector with image transducer; 1- laser light beam, 2 – acousto-optic transducer, 3 – optical system, 4 – polarization cube, 5 – image transducer, 6 – CRT, 7 – computer, 8 – photodiode, 9 – optical input.

Radar signal is compressed in optical correlator containing image transducer (see Fig. 18) and transformed into electric signal by photodiode. Input signal is transmitted to acousto-optical transducer made as Bragg cell. The first pair of lenses projects deflected beam at output surface of image transducer. Optical system of lenses passes only first order side beam of a signal. Signal of an adjusted mask is projected from CRT to input side of image transducer. Incident radar signal is correlated with reference mask represented in LC film by a measurement photocurrent of photodiode placed in zero order of space frequency of Fourier transformation. Photodiode signal is amplified and used in optical Doppler processor, which also contains image transducer. Laser beam is diffracted at acoustic wave generated by a signal in horizontal plane in acousto-optic transducer working as a processor input. The beam, after passing a horizontal deflector, is projected at an addressing input of image transducer. A deflector placed behind the acousto-optic transducer deflects beam vertically. An image obtained at the output is read by collimated beam of argon laser. Vertical transformation obtained by cylindrical lens and horizontal image allow to obtain an information concerning a distance and velocity of an object.

Nowadays the development of LCSLM's is very fast and promising [28].

3. Holography applications of liquid crystals

Hologram, in its simplest form, is in principle a kind of photography. The specific way of this photography consists in an information included into hologram, especially concerning phase and amplitude of transmitted or reflected light. For this reason, more competent information concerning registered object is included.

There are many different materials used for holograms making. The simplest one is photographic plate or foil of large resolution, on which an image of interferometric fringes originated from real object is registered. In this way hologram can be registered in a static way. The next stage is hologram read-out. The latter procedure consists in illumination of a hologram by coherent light and obtaining an image of a real object. As one can see, the stages of writing and read-out of a hologram are separated.

The most interesting is a situation when both above processes can be performed in the same time. This situation is called real-time holography [29]. Such an effect can be obtained, amongst others, using liquid crystals (LC) [30]. Typical set-up for real-time holography applying LC transducer is given in Fig. 19.

Light dividing plate BS divides laser light beam into two parts. The first one, so called object beam, incident optical system UO, which allows to illuminate an object P. The second one plays a role of a reference

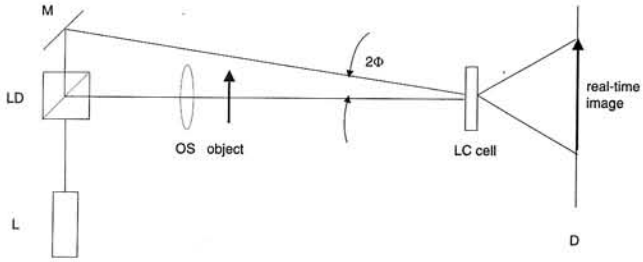

Fig. 19. Experimental set-up for real-time holography: L – laser, LD – light dividing plate, M – mirror, OS – optical system.

beam. Both beams are transmitted at LC transducer. As a result of an interference diffraction grating, constructed on local refractive and absorption coefficients, emerges. To obtain an image with good resolution changes of refractive and absorption coefficients should be so high to diffract at least one of the beams. Two waves A and B with wave vectors k_A and k_B, amplitudes A_A and A_B and intensities I_A and I_B form a diffraction grating. If an angle between beams is equal Φ, the wave vector of an obtained grating is given by an equation:

Grating period L is given by a formula:

$$\Lambda = \frac{2\pi}{q} \tag{24}$$

where q stands for a module of **q** vector.

Grating period can be also expressed as a function of an incidence angle Φ:

$$\Lambda = \frac{\lambda}{2n \sin\left(\frac{\pi}{2}\right)} \tag{25}$$

In case of small angles one can obtain:

$$\Lambda = \frac{\lambda}{n\Theta} \tag{26}$$

The smallest grating period can be obtained for light beam incident at 180° angle. Using visible light and a material with high Δn one can obtain Λ lower than 100 nm.

In practice each material, not only LC can be applied as a material for real-time image writing, because in each material Δn and $\Delta\varepsilon$ changes during such a situation, especially in case of photorefractive materials. Usually those changes are so small, however, that effective images cannot be obtained.

LC's allow to obtain real-time holograms without any developing process and for low-intensity read-out beam. One of the possible solutions is an application of a cell filled with dichroic dye-doped LC [31]. Such a cell consists of two glass plates with conductive and aligning layers. LC thickness from 10 to 100 μm is usually used. As a LC material typical LC mixture of $\Delta\varepsilon > 0$ with homogeneous alignment can be adopted. Such a mixture is usually doped by few tenths of weight per cent of light-resistant antraquinone dyes.

Dynamic process of a creation and vanishing of a hologram in an experiment of degenerated mixing of two light beams is presented in Fig. 20. Writing of a hologram requires an application of an electric field E, higher than threshold one, to the LC cell. For this reason a homeotropic alignment of LC containing dye is obtained. The proper conditions to write an image consist in an equilibrium between electric field and surface interactions of cell walls. The crucial role is played by sub-micron structures being a kind of domains. The key parameters of the system are speed of image writing and vanishing and reproducibility and efficiency of these processes. Till now an efficiency of first order diffraction is better than 30%, while writing times are order of 1 ms. During image vanishing one of beams is blocked.

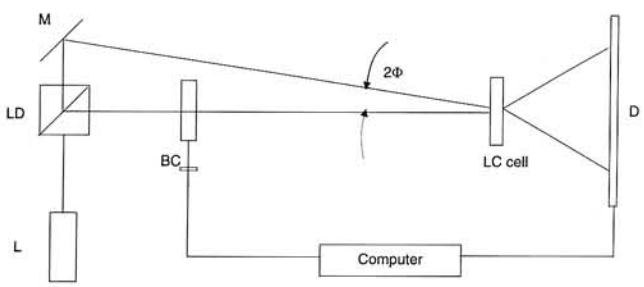

Fig. 20. Dynamic process of a creation and vanishing of the hologram during degenerated mixing of two beams; BC – beam cracker.

Vanishing of a hologram can be performed not only by an elimination of one of beams but also by voltage switch-off, however the latter process is much slower. The largest efficiency can be obtained if a polarization direction of an incident beam coincides rubbing direction at a cell wall. The mechanism of hologram emerging in LC structures is connected with induced photoconductivity [33].

Holograms in LC systems allow to obtain new applications, e.g. holographic memory, optical correlators, optical transistors and holographic movies.

4. Liquid-crystal waveguides

One of the most interesting applications of optical signals processing are LC integrated optics systems. In a waveguide system, in which guiding layer is made of LC, a detection or modulation of light can be obtained. [34]. To drive changes of LC refractive index electro- or acousto-optical effects can be adopted. The general scheme of a deflection of light beam in acousto-optic version of a device is presented in Fig. 21.

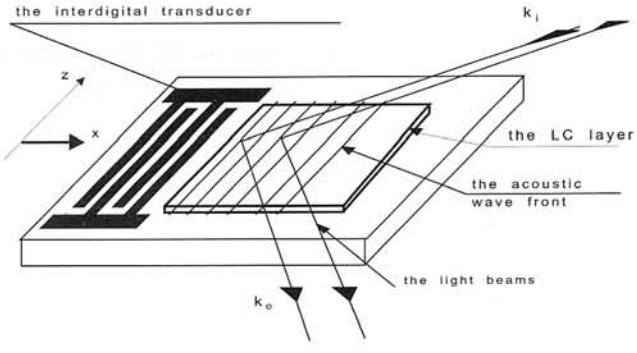

Fig. 21. Scheme of interactions during a modulation of electromagnetic wave guided by surface acoustic wave.

In this Figure interactions connected with modulation of electromagnetic wave guided in LC layer by surface acoustic wave (AFP) is presented. Surface wave is generated in piezoelectric substrate by interfinger transducer. LC layer is made in this way that may act as a waveguide for electromagnetic wave. An introduction of light into LC waveguide is based on an application of prismatic grating couplers and suitable optical microsystems based on laser diode and allowing to introduce wave directly from waveguide front. [35]. Prismatic couplers act on the base of tunneling coupling of incident wave with waveguide modes guided in LC layer placed at one of prism walls. They are made of materials with high refractive index, while waveguiding LC layer is placed between layers of refractive indices lower than LC ordinary refractive index. The thickness of such an optical buffer should be calculated in a suitable way [36].

Electric driving in a system shown in Fig. 21 is obtained by an application of typical transparent conductive oxide electrodes applied at the waveguiding path. Electric field cause uniform distribution of refractive index in waveguiding layer. As a result of an interaction of waveguiding mode with non-uniformities of refractive index one can obtain a diffraction of guided wave.

In a construction of such devices one can find, apart of advantages, also the following difficulties:

- methods of an introduction and getting out of electromagnetic wave to and from LC waveguiding layer,
- preserving a suitable collimation of light beam for Bragg regime,
- minimization of AFP damping under LC layer,
- minimization of waveguiding modes damping

The third of enlisted problems has been described in [37-39]. Chosen elements of an AFP application in waveguide adopted for acousto-optic modulation have been presented there. The special attention has been paid to surface transverse (STW) and Stoneley waves. The best results of acousto-optic driving are obtained for Stoneley wave propagating on the border between LC and elastic substrate.

Very difficult task is a light beam forming to introduce it into optic fiber and obtain low beam refraction in waveguide plane. The technology of beam forming is crucial for a parameters of deflector construction. Using Bragg effect one should remember that beam parallelity affects parameters of waveguide deflector.

An application of waveguide deflector is limited to processing of low-power light signals due to nonlinear effects in LC layers. Usually source power up to 10mW has been used.

Technique of an introduction of light beam into LC layer affects energy losses; usually losses order of 1dB/cm have been observed. When unpolarized light is used for an excitation losses over 10dB/cm are observed [40]. However, it is possible to obtain reproducible losses order of 3dB/cm [38].

The special area of an application of LC waveguides are studies of LC material parameters. Typical techniques used in solid state physics have been adopted for this purpose (attenuated total reflection or total reflection). Those methods can be improved by integrate optics techniques [41-43]. In mentioned works measurement head build of two prism couplers with LC waveguide between them has been adopted [6]. The method of measurement of refractive index profile allows to obtain a local optical axis in transversal cross-section of a waveguide [42]. Results of measurements obtained by this method allow to find elastic interaction between LC and a substrate [38].

Acknowledgement

This work has been supported by Committee for Scientific Research grant no. 8S 501 049 07.

References

1. Gniadek, *Optyczne przetwarzanie informacji*: Wyd. Naukowe PWN Warszawa (1992).
2. J. W. Goodman, *Introduction to Fourier Optics*: Mc Graw – Hill, New York (1968).
3. P. M. Duffiax, *The Fourier Transform and its Application to Optics*: Wiley, New York (1983).
4. J. A. Neff, R. A. Athale and S. H. Lee, Proc. of the IEEE **78** 826 (1990).
5. A. D. Fisher, Int. J. Optoelectronics **5** 125 (1990).
6. B. Bahadur, Liquid Crystals, *Applications and Uses,* Vol. 3 World Scientific (1992).
7. J. Żmija, J. Zieliński, J. Parka and E. Nowinowski – Kruszelnicki, *Displeje ciekłokrystaliczne. Fizyka, Technologia, zastosowanie*: Wyd. Naukowe PWN, Warszawa (1992) (in Polish).
8. J. Żmija, S. Kłosowicz and W. Borys. *Cholesteryczne ciekłe kryształy w detekcji promieniowania*: WNT Warszawa (1989) (in Polish).
9. J. W. Goodman, A. R. Dias and L. M. Moody, Opt. Lett. , **2** 1 (1977).
10. O. V. Garibyan, I. N. Kompanets, A. V. Parfenov, N. F. Pilipetsky, V. V. Shkunov, A. N. Sudarkin, A. V. Sukhov, N. V. Tabirian, A. A. Vailiev and B. Ya. Zel'dovich. Opt. Comm. **38**, 67 (1981).
11. E. Marom, V. Efron, Opt. Łett. **12** 504 (1987).
12. K. M. Johnson, C. C. Mao, M. A. Handschy, K. Amett and G. Moddel, Opt. Lett. **15** 1114 (1989).
13. T. Lagerwall, N. A. Clark, J. Dijon and J. F. Clerc, Ferroelectrics **94** 3 (1989).
14. J. A. Raalte Proc. IEEE **56** 2146 (1968).
15. H. K. Liv and T. H. Chao, Appl. Opt. **28** 4779 (1989).
16. D. Armitage, J. I. Thackara and W. D. Eades, Appl. Opt. **28** 4763 (1989).
17. M. Pluta, *Mikrointerferometria w świetle spolaryzowanym*: WNT, Warszawa, 1991 (in Polish).
18. J. Kędzierski, *Elastyczność, podatność diamagnetyczna i potencjał oddziaływania nematyków z podłożem*: Warszawa WAT 1994 r (in Polish).
19. N. F. Kovtonyuk and V. V. Bielyaev. Proc. SPIE, **2051** 254 (1993).
20. V. V. Belyaev and V. G. Chigrinov, Appl. Opt. **32** 2, 141, (1993).
21. C. S. Sexton, Proc. SPIE **684** 96 (1986).
22. M. H. Wu (Hamamatsu Corp.) private information
23. P. Morlenson, Laser Focus World **18** 25 (1992).
24. K. Takizawa, H. Kikuchi, H. Fujikake, T. Fujii, M. Kawakita and M. Yokozawa, Proc. SPIE, **2407** 136 (1996).
25. T. Fujii, H. Kikuchi, M. Kawakita, H. Fujikake and K. Takizawa, SID Proceedings, Eurodisplay'96, 80 (1996).
26. S. J. Kłosowicz, Opto-Electronics Review, **2'93** 58 (1993),
27. D. G. Siharulidze, G. S. Chilaya, M. I. Brodzeli, Kwantowaja Elektron **6** 1271 (1979).
28. See, e. g. session 7 of Projection Display Proceedings, Proc. SPIE, **2407** 198-235 (1995).
29. H. J. Eichler, P. GĆnter, and D. W. Pohl, *Laser Induced Dynamic Gratings*: Berlin, Springer Verlag, 1986.
30. I. C. Khoo, *Liquid Crystals Physical properties and Nonlinear Optical Phenomena*: New York, Wiley, 1995.
31. I. Janossy, Phys. Rev. E, **49** 2957 (1994).
32. S. Kłosowicz, E. Nowinowski, Z. Raszewski, A. Walczak, J. Zieliński and J. Żmija, Journ. Techn. Phys. **35** (4) 363 (1994).
33. A. Miniewicz, S. Bartkiewicz, A. Januszko and J. Parka, Photoactive Organic Materials Science and Application, Dordrecht, Kluwer Academic Publishers, 1996.
34. S. Kłosowicz, E. Nowinowski, Z. Raszewski, A. Walczak, J. Zieliński and J. Żmija, Journ. Techn. Phys. , **35**(4), 363-369 (1994)
35. A. Walczak and J. Żmija, *Nonlinear Optics of Liquid Crystals*: Conference Proc., Crimea, 1992
36. A. Kieżun, L. R. Jaroszewicz, E. Nowinowski – Kruszelnicki and A. Walczak: Polish Patent Application P-310. 765, 29. 09. 95
37. A. Walczak, Proc. SPIE. **1845** 362 (1992)
38. A. Walczak, World Congress on Ultrasonics Berlin Proc. , Sept. 1995, 399
39. E. Nowinowski-Kruszelnicki, A. Walczak, A. Kieżun and L. R. Jaroszewicz, ECLC97, Conference, Zakopane 97, Proc. SPIE, (1997) in print.
40. A. Walczak, Bull. WAT, **3** 103 (1997).
41. E. Nowinowski-Kruszelnicki, A. Walczak, A. Kieżun, L. R. Jaroszewicz, ECLC97 Conference, Zakopane 97, SPIE Proc. , 1997, in print
42. A. Walczak, A. Kieżun, E. Nowinowski-Kruszelnicki, L. R. Jaroszewicz: *Application of Planar Wavequide Technique to Investigation of Liquid Crystals*: Electronics and Telecomunications Quarterly, **42** (3) 335 (1996).

